COMPARISON OF PHOTOCATALYTIC ACTIVITY OF ZINC OXIDE AND IRON OXIDE NANOPARTICLES TOWARDS DEGRADATION OF PHENOL RED ORGANIC DYE

GADEGONE S.M.[1], BARVE A.K.[1], LANJEWAR M.R.[2] AND LANJEWAR R.B.[3]

[1.] Kamla Nehru Mahavidyalaya, Sakkardara, Nagpur.

[2.] Department of Chemistry, R.T.M Nagpur University, Nagpur.

[3.] Dharampeth M.P. Deo Memorial Science College, Nagpur.

mail id :sunita.gadegone@gmail.com

Abstract: The photocatalytic activity of zinc oxide and iron oxide nanoparticles was studied at different pH. The microstructure properties of both samples were characterized by XRD, FTIR and TEM. The average particle size of ZnO and Fe_3O_4 was 20 nm and 10 nm. Kinetics of disappearance of phenol red in aqueous solution was used as test reaction and found that ZnO exhibited good photocatalytic efficiency at acidic condition.

Keywords: ZnO, Fe_3O_4, degradation, photocatalytic activity

INTRODUCTION:

Nanotechnology is an emerging field that covers a wide range of technologies which are presently under development in nanoscale. One of the important applications of nanotechnology in the field of environmental factors is the remediation of water, prevention of pollutants, removal of toxic elements, etc. Because of the rapid development of industries, there occurs a contamination of dye pollutant in the environment (Zhong, 2007). Among various physical and biological techniques for the treatment of pollutants, precipitation, adsorption, air stripping, flocculation, reverse osmosis, and ultra-filtration can be used for color removal from textile effluents (Robinson et al., 2001 and Paula et al., 1998). Phenol contamination can cause toxic effects on aquatic flora and fauna as well as human beings. Phenols are toxic to human beings and affect several biochemical functions (Nuhoglu and Yakin, 2005)

In the described work below, the ZnO and Fe_3O_4 nanoparticles were used for photocatalytic oxidation of phenol red organic pollutant. Such treatment has the advantage that the size of particles is affected by the ratio of surfactant to water.

MATERIALS AND METHODS :

Synthesis: Phenol red and Zinc acetate are of AR grade purchased from Merck. Ferric chloride and ferrous sulphate was purchased from Himedia India. The procedure has been carried out for the degradation of organic pollutant at different pH = 2, 4, 6, 8, and 10. The concentration of pollutant was taken to be 10 ppm and that of nanocatalyst was 1 mg/lit. After that, the suspension was stirred in the dark for 1 hour in order to achieve the absorption phenomenon at that particular pH. The initial absorbance was noted to be as A_o. The absorbance at 0 min was noted and then the sample was irradiated under UV radiation for 30 min with constant aeration. The procedure was continued for 3 hours at a time interval of 30 min. After each interval, the absorbance was noted as a function of time.

RESULTS AND DISCUSSION :

XRD:

All the diffraction peaks of Fig. 1. can be assigned to cubic Fe_3O_4 with $2\theta = 18.43^o, 30.29^o, 35.62^o, 43.29^o, 53.53^o, 59.36^o, 62.86^o$ and 74.41^o corresponds to the (111), (220), (311), (400), (422), (511), (440) and (533) crystal plane.It is found that the position and relative intensity of the XRD peak patterns match well with the standard magnetite samples according to JCPDS cards No. 85-1436. These indicating the samples are in inverse spinel structure with a face-centered cubic phase. The mean crystallite size of the sample is determined by using the Debye-Scherrer's formula and calculated to be 10 nm.

While in Fig.2 shows the XRD patterns of ZnO nanocrystalline powder. All the diffraction peaks are assigned to well indexed to the crystalline hexagonal phase of the ZnO nanomaterial, with lattice constants of a=1.8144Å, d=1.283 Å. The XRD peaks of ZnO is found to be (101), (102), (110) and (200) at a diffracting planes at $2\theta = 35.88^o, 47.28^o, 56.28^o$, and 62.53^o respectively indicating the formation of phase pure wurtzite structure of ZnO (JCPDF 79-0208).

TEM:

From the Fig. 3, it is clear that the nanoparticles are elongated rod shaped with a narrow size distribution and agglomeration and their particle size is 7.85 nm in accordance with the XRD (10 nm) and suggest that each particle is a single crystal. From the image, it is clearly seen that the distribution of the particles was not uniform but form weak agglomeration. Since the magnetite exist in inverse spinal structure with a unit cell consisting of 32 oxygen atoms in a face-centered cubic structure and a unit cell edge length of 8.390Å. In this crystal structure Fe(II) ions and half of the Fe(III) ions occupy octahedral sites and half of the Fe(III)occupies tetrahedral sites. The TEM image clearly reveals the inverse spinel structure of the nanomaterial. The SAED pattern also confirms the presence of inverse spinal structure of the magnetite nanoparticle synthesized by microwave method. From the electron diffraction pattern, the particles give clear

diffraction circles that are typical for random oriented and well-defined polycrystalline particles.

Fig.4 shows the TEM image of synthesized ZnO nanoparticles. The ZnO particles are nearly spherical in shape with more agglomeration. The ZnO prepared by this method are rather well separated with an average size of approximately 10-15 nm which is in good agreement with the grain size calculated by Debye-Scherer formula. In the same figure shows the corresponding diffraction pattern of ZnO nanoparticles which also confirms the cubic phase structure of the sample. The image shows the ring pattern of the ZnO which indicates the peak positions obtained in the X-rays diffraction pattern. ZnO nanomaterial with average size of 10 nm has also been confirmed (Jayaraj, 2009).

Photocatalytic activity:

Nanomaterial of Fe_3O_4 is a low-cost, recollectable and stable photocatalyst for the degradation of organic dye. This is due to the high surface area and well defined pore size, which also enhances their photocatalytic activity. The particle size of nanomaterial also has an effect on the energy level of the photocatalyst. Fig 5. depicts the photocatalytic activity of Fe_3O_4 nanomaterial for the degradation of phenol red in aqueous solution under UV light irradiation at different pH values.

From the Fig 5 and 6 it was found that, the decolourization of the dye is found to be unsusceptible to higher pH. Hence at acidic range of pH, the surface of the particle is positively charged and at alkaline range of pH, it is negatively charged (Guillard, 2003). The decrease in degradation at higher pH value may be due to the fact that phenol red is an anionic dye and at higher pH there may be repulsion between the charges of the dye molecules as well as the Fe_3O_4 nanoparticles. The interpretation of pH effect on the efficiency of the photochemical process is a very tedious task, because three possible reaction mechanisms can contribute to dye degradation, namely: hydroxyl radical attack, direct oxidation by the positive hole and direct reduction by the electron in the conduction band. The importance of each one depends on the substrate nature and pH (Tang, 1997).

At pH 2, the degradation percentage was 71.43% showing that for a better degradation of the pollutant, it is essential to maintain the lower pH. In acidic pH, the photo excited electrons in the photocatalyst could be fast abstracted from the surface by the numerous protons of the medium.

The Langmuir-Hinshelwood model can be used to describe the relationship between the rates of the photocatalytic degradation of dye in the presence of Fe_3O_4 as a function of irradiation time. The plot of the logarithm of the ratio between the initial concentration of phenol red dye and the concentration after photocatalytic degradation ($\log C_0/C$) versus the corresponding irradiation time (min) yields a linear relationship as shown in Fig.6. Pseudo-first order rate constants were evaluated from the slope of the plots between log (C_0/C) and time and the plots were found to be linear in accordance with L-H model with positive slope.

The pseudo-first-order rate constants with different pH = 2, 4, 6, 8 and 10 of phenol red are found to be 5.93×10^{-3}. The k values are found to be constant with the increase in pH values suggesting first-order dependence of the reaction rate on dye. Therefore, the photocatalytic degradation reaction of phenol red dye by Fe_3O_4 belongs to the pseudo-first-order reaction kinetics.

It is clear that Fe^{3+} carries more positive charges in acidic solution while at higher pH Fe^{3+} might carry negative or neutral charges. Hence, at alkaline condition nanoparticles show less adsorption of organic pollutant while for acidic condition, there is slight increase in degradation of pollutant.

Plots of percent degradation of phenol red as a function of reaction pH using same concentration of phenol red dye as 10 ppm and ZnO catalyst load are shown in Fig.7 and plots for degradation percentage of dye as a function of irradiation time for the above system is given in Fig. 8. It is observed that percentage degradation of phenol red increases when pH is 2 but at higher pH the degradation of the dye is gradually decreased. Above pH, 7, the photocatalytic degradation of phenol red rapidly decreases. This may be due to the existence of negative charge at the surface of ZnO photocatalyst due to the adsorbed OH^- ions. Since the point of zero charge of ZnO is pH = 7 and the adsorption of negatively charged phenol red on the photocatalyst surface is repelled and hence a decrease in the observed photocatalytic degradation. The ionization state of the surface of the photocatalyst can be protonated and deprotonated under acidic and alkaline conditions, respectively, as shown in the following equations:

$$ZnOH + H^+ \rightarrow ZnOH_2^+$$
$$ZnOH + OH^- \rightarrow TiO^-H_2O$$

The ZnO can act as a trap for photo-excited electrons that lengthens the lifetime of charge carrier's results in enhanced photocatalytic activity of ZnO. Photocatalytic degradation rate constant (k) of the PR dye was calculated using Langmuir-Hinshelwood first order kinetics.

In general, the protonation and deprotonation can be explained in terms of species specification conditions. For an organic compound that undergoes protonation/deprotonation reactions, the pH change will influence not only their absorbed quantity but also specific complexion modes i.e. adsorbate co-ordinate to ZnO surface. Hence, pH will influence the photocatalytic oxidation kinetics of strong adsorbate particles. Also, the band energy of ZnO will change with pH and thermodynamically this change directly leads to change in the oxidation power. At lower pH, the adsorption is decreases and rate determining step for photocatalytic degradation of phenol red is the surface reaction step after absorbed ZnO nanoparticles. Hence photocatalytic reaction is faster at lower pH range because the net reaction consumes the protons (Thakare, 2003).

CONCLUSION :

From the results obtained, zinc oxide and magnetite nanocatalyst are efficient for the photodegradation of phenol red under the influence of UV-Visible radiation. Photocatalytic reduction is higher for the solution having pH 2. Both the nanocatalyst reduces the dyes at acidic range. Comparatively, ZnO provides excellent degradation under acidic conditions.

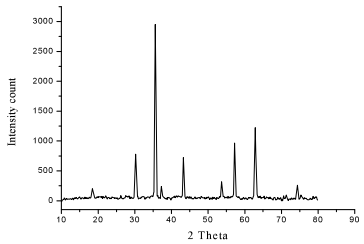

Fig. 1. XRD pattern of Magnetite

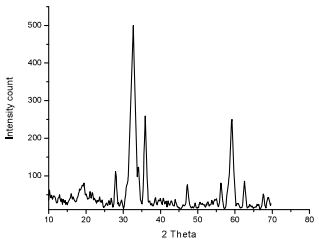

Fig. 2 XRD pattern for ZnO nanoparticle

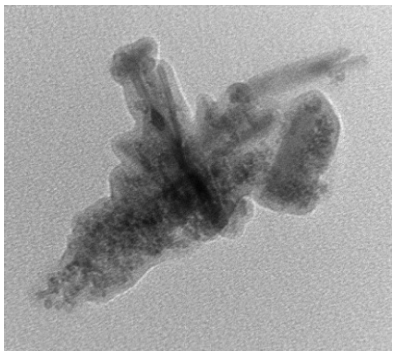

Fig. 3 TEM image for Magnetite nanoparticle

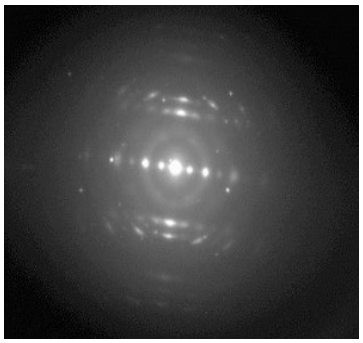

Fig. 4 SAED pattern for Magnetite nanoparticle

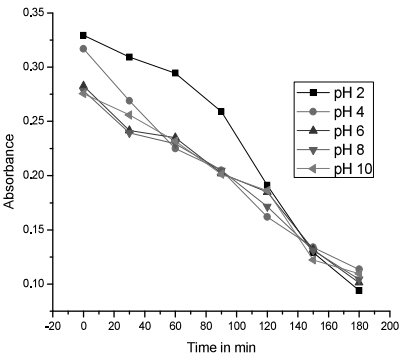

Fig.5.Depletion of Absorbance with respect to time

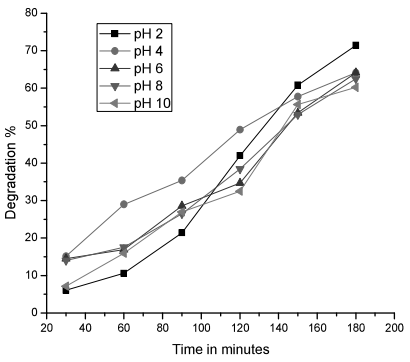

Fig.6. Degradation percentage of Phenol red against time

REFERENCES:

1. **A. Nuhoglu and B. Yakin** "Modeling of phenol removal in a batch reactor*" Process of Biochemistry* **40**, 233-239, 2005.
2. **H. Guillard et al.**, "Influence of chemical structure of dyes, of pH and of inorganic salts on their photocatalytic degradation by TiO_2" & "Comparison of the efficiency of powder and supported TiO_2" *J. Photochemistry Photobiology A: Chemistry,* **158**, 27-36, 2003.
3. **M. Jayaraj, P. Aneesh and K. Vanaja** "Synthesis of ZnO nanoparticle by hydrothermal method" *Nanophotonic Materials IV, edited by Zeno Gaburro, Stefano Cabrini, Proc. of SPIE* **6639-66390J**, 2009.
4. **M. Paula, S. Van and L. Y. Young** "Isolation and Characterization of phenol degrading denitrifying bacteria" *Applied and Environmental Microbiology* **64**, 2432-2438,1998.
5. **R. Robinson, G. McMullan, R. Marchant and P. Nigam** *Bioresource Technology* **77,** 25, 2001.
6. **S. Thakare and R. Jugele**, *Ind. J. of Chem.* **42A** , 513-515, 2003.
7. **W. Z. Tang, Z. Zhang, H. An, M. O. Quintana, D. F. Torres** "TiO_2/UV photodegradation of azo dyes in aqueous solutions". *Environ. Technol. Vol.* **18,** 1- 12, 1997.
8. **X. J. Zhong, L. Zhang and D. L. Li** "Degradation of 4-toluene sulphonic acid by photocatalysis of nano TiO_2" *Acta Scientiae circumstantial* **27,** 1835-1839, 2007.

CRYSTAL STRUCTURE Ti DOPED Alq_3 BLUE OLED ORGANIC NANO PHOSPHOR

SUNIL A BHAGAT
Department of Physics
Kamla Nehru Mahavidyalaya, Nagpur, 440024
Sunilbhagat15@rediffmail.com

Abstract: Titanium doped alumium-8-hydroxyquinoline metal complex has been synthesized by simple precipitation route in order to reduce the cost and time of synthesized material. It is characterized by XRD. X-ray Diffractogram of Ti doped Alq_3 complex displays well defined X-ray diffraction lines, confirming its crystalline nature. The X-ray diffraction data analysis is done which confirms the formation of nano size crystal structure. The synthesized Ti doped Alq_3 organic nano phosphor is promising material for optical or optoelectronic applications.

Keywords: nano phosphor, Alq_3, Xrd, Ti doped Alq_3

INTRODUCTION:

Now a days Organic light-emitting diodes (OLEDs) constitute a rapidly developing field. Many believe that they represent the future of flat panel display technology. The main focus of OLED research is to address these issues. Two types of compounds: conjugated organic polymers, such as poly (1, 4-phenylenevinylene) (PPV) and molecular species such as aluminum tris-(8-hydroxyquinolate) (Alq_3) are used frequently. Organic have attracted tremendous interests for application in functional nanoscale electronic and optoelectronicdevices, the crystallinity and molecular arrangement of which have a great influence on the performance of these devices. [1–4] However, compared with the overwhelming majority of inorganic nanomaterials, only a few successful preparations of organic one-dimensional (1D) nanomaterials such as nanowires and nanotubes are reported. [3, 5–7]**.** Since the first efficient low-voltage-driven organic light-emitting diodes (OLEDs) based on tris(8-hydroxyquinoline)aluminium(Alq_3) were reported [8]. Alq_3 has become a important prototypical electron transport and emitting material for OLED devices because of its excellent stability and electro-luminescence properties. Therefore lumophores based on Aluminium metallo-8-hydroxyquinolate prepared from wet Chemical method and co-doped with Titaniumtransition element is prepared and characterization of the material by X-Ray diffraction spectrographic is done. Alumium-8-hydroxyquinoline and co-doped materials with varying concentrations of dopants are synthesized by simple wet Chemical route in order to reduce the cost and time of synthesized material. In the synthesis technique when Ti transition metal is added which contribute an electron, withdrawing constituent at the 5-position in 8-hydroxyquinoline, increasing the solubility of the corresponding metal quinolate complexes in non polar solvents produces an intense green-emission at the excitation around 435-440 nm wavelength (i.e. violet OLED excitation wavelength).

MATERIALS AND METHODS :

Alq_3 was prepared as follows: firstly take 25 ml double distilled water and 25 ml acetic acid in beaker. Dissolve 5 gm of 8-hydroxyquinoline in a mixture of double distilled water, acetic acid and stir it still the orange transparent solution was obtained say solution I. Take 4.3069 gm Al $(NO_3)_3.9H_2O$ and dissolve in double distilled water. Stir it till clear solution was obtained say solution II. Mix the solution I and II and stir for 10 min and add N_4OH solution by drop by drop to this mixture of solution with continuous stirring. Filter the yellow green precipitate and wash the precipitate with double distilled water for 8 to 10 times. Place the precipitate for drying 40-50^{o}C. The other derivative of 8-hydroxyquinoline metal complex is prepared by Simple precipitation method same as Alq_3. Aluminum nitrate is replaced by nitrates of those metals. For the preparation of Alq_3 host lattice, aluminum nitrate and 8-hydroxyquinoline as raw materials and for Alq_3: Ti, Titanium oxide is used as other material mixed in an appropriate molar ratio. The synthesis chemical reactions as follows

$$Al(NO_3)_3.9H_2O + (C_9H_7NO) \rightarrow Al(C_9H_7NO)_3 + 9H_2O + 3(NO_2)\uparrow$$

$$Al(NO_3)_3.9H_2O + TiO_2 + 7(C_9H_7NO) \dashrightarrow Al\,Ti(C_9H_7NO)_7 + 9H_2O + NO_2\uparrow$$

RESULTS AND DISCUSSION :

XRD OF Alq_3: Ti

Diffraction data has historically provided information regarding the structures of crystalline solids. Such data can be used to determine molecular structures, ranging from Simple to complex, since the relative atomic positions of atoms can be determined. X-ray Diffraction provides important evidence and indirect proof of atoms. The Symmetry of the diffraction patterns corresponds to the symmetry of the atomic packing. It is the simplest way to determine the inter atomic lattice spacing that exists. The intensity of the diffracted beams also depends on the arrangement and atomic number of the atoms

in the repeating motif, called the unit cell. Thus, the intensities of diffracted spots calculated for trial atomic positions can be compared with the experimental diffraction intensities to obtain the positions of the atoms themselves. The XRD pattern did not indicate presence of the constituents like nitrates, ammonia and other likely phases. This result indicates whether the final product formed is in crystalline and homogeneous form or not. The particle size is calculated and reported in this paper. The synthesized complex have been characterized by XRD on the 'Expert pro' Automated power Diffractometer system company name Analytical, Netherland taken at 'SAIF' Punjab University, Chandigarh.

Measurement Conditions for particle size of Alq_3: Ti
Calculation of xrd peaks
The calculations is carried out by Scherer's formula

$D = 0.9 * \lambda/\beta \cos(\theta)$ (λ=1.54A)

To calculate the first peak

2θ= 10.2648, θ=5.1324
β=0.0669 x3.14/180 = 0.00116703 =1.1670 x 10^-3(in radian)
D_1= 0.9x 1.5406x10^-10/1.16703x10^-3x cos (5.1324)
D_1 =118.32 nm

To calculate the second peak

2θ =14.2065, θ =7.10325
β =0.1004 x3.14/180 =1.7514 x10^-3 (in radian)
D_2= 0.9 x 1.5406 x10^-10/1.7514 x10^-3 cos (7.1147)

D_2=78.55nm

Similarly, calculations for all other peaks is as follows 96.17 (nm), 80.51(nm), 67.58 (nm), 46.57(nm), 79.17(nm) The average grain size of crystallites is found to be D = 80.9814(nm). Further investigation on the grain size of this complex by SEM should be carried out.

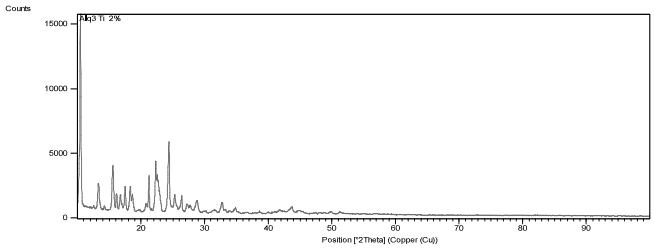

CONCLUSION

Alq_3: Ti hybrid organic complex has been synthesized by the precipitation wet chemical method and characterized by XRD spectrograph. X-ray spectrograph of Ti doped Alq_3 complex displays well defined X-ray diffraction lines, confirming its crystalline nature and grain size is calculated to be 80.98nm in the nano range. Further investigation on the particle size of this complex by SEM should be carried out. Hence the organic nanophosphor i.e. Alq_3: Ti is suitable for PLLCD and OLED, nanorods, nanowires and solid state lighting application devices.

Fig. 1: XRD OF Alq3: Ti

Table1: Peak List

Pos. [°2Th.]	FWHM [°2Th.]	d-spacing [Å]	Rel. Int. [%]	Area [cts*°2Th.]
10.2648	0.0669	8.61790	27.82	284.45
10.4689	0.1338	8.45031	100.00	2045.04
12.5373	0.1004	7.06048	4.14	63.47
13.2961	0.1428	6.65370	15.04	443.61
13.3622	0.1020	6.63736	13.83	291.46
14.2467	0.2040	6.21178	4.00	168.70
15.4975	0.1224	5.71313	20.71	523.52
15.5860	0.1428	5.68090	24.23	714.79
16.1697	0.1836	5.47711	10.36	393.04
16.7789	0.1224	5.27959	9.15	231.25
17.5058	0.2040	5.06197	13.64	574.62
18.3083	0.2040	4.84188	13.56	571.36
18.7219	0.1224	4.73583	8.46	213.94
19.7484	0.2448	4.49192	1.97	99.69
20.7752	0.1836	4.27217	5.16	195.84
21.2577	0.1836	4.17627	19.15	726.29
22.3062	0.1224	3.98228	26.41	667.60
22.5517	0.1428	3.93948	19.31	569.57
22.7077	0.1224	3.91278	16.70	422.10
24.3596	0.2244	3.65105	36.00	1668.82
25.3204	0.1428	3.51464	9.63	284.09
26.3740	0.2040	3.37659	8.94	376.59
27.2277	0.3672	3.27262	5.09	385.81
27.7475	0.2448	3.21247	4.05	204.73
28.7642	0.2856	3.10120	6.61	390.22
30.1737	0.1632	2.95947	1.51	50.79
31.5260	0.7344	2.83554	1.84	279.30
32.7562	0.3264	2.73180	5.49	370.30
33.2515	0.2448	2.69223	2.20	111.45
33.8948	0.2448	2.64259	1.59	80.57
34.8479	0.1632	2.57247	2.93	98.74
36.5516	0.8160	2.45638	0.60	101.10
38.5846	0.1632	2.33150	1.19	40.21
39.9992	0.4080	2.25225	0.75	63.15
41.8028	0.3264	2.15915	1.86	125.21
43.6683	0.2448	2.07114	3.39	171.42
44.8205	0.4080	2.02053	1.71	143.75
45.3759	0.3264	1.99708	1.28	86.22
48.2165	0.4896	1.88585	0.63	63.98
49.8308	0.4896	1.82847	1.00	100.92
51.2372	0.4080	1.78154	0.86	72.15
56.6759	0.6528	1.62281	0.34	45.93

REFERENCES :

1. J. G. C. Veinot and T. J. Marks, Acc. Chem. Res., 2005, 38, 632.
2. J. J. Chiu, C. C. Kei, T. P. Perng and W. S. Wang, Adv. Mater., 2003,15, 1361.
3. H. B. Liu, Q. Zhao, Y. L. Li, Y. Liu, F. S. Lu, J. P. Zhuang, S. Wang,L. Jiang, D. B. Zhu, D. P. Yu and L. F. Chi, J. Am. Chem. Soc., 2005,127, 1120.
4. M.Kastler,W.Pisula,F. Laquai, A.Kumar,R.J.Davies,S. Baluschev,M. C. Garcia-Gutie ´rrez, D. Wasserfallen,H. J.Butt, C. Riekel,G. Wegner and K. Mu ¨llen, Adv. Mater., 2006, 18, 2255.
5. H. B. Fu, D. B. Xiao, J. N. Yao and G. Q. Yang, Angew. Chem., Int.Ed., 2003, 42, 2883.
6. J. S. Hu, Y. G. Guo, H. P. Liang, L. J. Wan and L. Jiang, J. Am. Chem.Soc., 2005, 127, 17090.
7.J. K. Lee, W. K. Koh, W. S. Chae and Y. R. Kim, Chem. Commun.,2002, 138.
8. C. W. Tang and S. A. Van Slyke, J. Appl. Phys., 1989, 3610.